European Drag Reduction and Flow Control Meeting – EDRFCM 2017
April 3–6, 2017, Rome, Italy

REYNOLDS NUMBER DEPENDENCE OF LARGE-SCALE FRICTION CONTROL IN TURBULENT CHANNEL FLOW

J. Canton[1], R. Örlü[1], Cheng Chin[2] and P. Schlatter[1]
[1]Linné FLOW Centre, KTH Mechanics, Royal Institute of Technology, Stockholm, SE-100 44 Sweden
[2]Dept. of Mechanical Engineering, The University of Adelaide, Adelaide, South Australia 5005 Australia

INTRODUCTION

The search for an effective mean of reducing turbulent skin-friction drag is one of the most active fields of research in fluid mechanics. The benefits of efficient flow control are numerous: from energy and economical savings, to more efficient and greener machinery, be it aviation or fluid transport and mixing [5]. Several techniques have been investigated, ranging from passive methods such as riblets [6], to active control strategies as, for example, streamwise-travelling waves of spanwise wall velocity [15], uniform blowing and suction [10], volume forcing [13], and direct modification of the mean flow [16]. Most of these control techniques, though, have been analysed only at low Reynolds numbers (Re) and only recently some authors have started investigating the effects that an increasing Reynolds number has on the flow control strategy (see, for instance, Refs. [9, 8, 7]).

One of the more promising techniques consists of the large-scale vortices proposed by Schoppa & Hussain [16] which (in the original study) were embedded in a turbulent channel flow at a friction Reynolds number $Re_\tau = 104$, where turbulence is marginally sustainable. This drag reduction strategy was found to be ineffective by Canton *et al.* [1], since the claimed drag-reduction effect was shown to be of transient nature. Nonetheless, Canton *et al.* [1] recast the method as a volume forcing control for channel flows that lead to sustainable drag reduction at $Re_\tau = 180$. These large-scale vortices were promoted by their original authors as a promising, feed-forward or passive, control technique capable of reducing the turbulent friction drag from the outside of the viscous layer, and thus independent of the small scales of wall turbulence, which would otherwise limit its applicability at practically relevant Reynolds numbers due to sensor/actuator limitations [11].

It is well known, though, that near-wall structures scale with viscous units (see *e.g.* Ref. [12]) and that low Reynolds number effects are present in wall-bounded flows at least up to $Re_\tau = 395$ [14]. Moreover, it has been found that the performance of different control strategies deteriorates as the Reynolds number is increased; this is the case at least for the active V- and suboptimal control schemes [9] and the oscillating wall and travelling waves [8, 7]. These two observations provide the main motivation for the present analysis.

NUMERICAL SETUP

This work is concerned with direct numerical simulations (DNS) of incompressible channel flows at fixed bulk Reynolds number Re_b, based on bulk velocity U_b, channel half-height h and fluid viscosity ν. Four values of bulk Reynolds number are employed: $Re_b = 1518, 2800, 6240$ and 10000, such as to result in a friction Reynolds number, based on friction velocity u_τ, h and ν, corresponding to $Re_\tau \approx 104, 180, 360$ and 550, where the lowest Reynolds number corresponds to the value employed in the original study by Schoppa & Hussain [16]. The simulations are performed using the pseudo spectral code `SIMSON` [3]. Details of the domain sizes and spatial resolutions used for the four sets of simulations are reported in table 1.

Re_τ	Integration time $T \cdot [h/U_b]$	Domain size $L_x/h,\ L_z/h$	Grid points $N_x,\ N_y,\ N_z$
104	10500	8, 3.832	48, 65, 48
		8, 6.6	48, 65, 60
		8, 9.9	48, 65, 96
180	1500	12, 6.6	128, 97, 96
		12, 9.9	128, 97, 144
360	1000	12, 6.6	300, 151, 200
		12, 9.9	300, 151, 300
550	400	12, 6.6	432, 193, 300

Table 1: Details of the numerical discretisation employed for the present simulations. T corresponds to the duration of the controlled simulations; N_x and N_z represent the number of Fourier modes employed in the wall-parallel directions (values before dealiasing), while N_y is the order of the Chebyshev expansion used for the wall-normal direction.

The large-scale vortices, provided with variable intensity and spanwise wavelength, are imposed via a volume forcing defined as:

$$\begin{aligned} f_x &= 0, \\ f_y(y,z) &= A\beta \cos(\beta z)(1+\cos(\pi y/h)), \\ f_z(y,z) &= A\pi/h \sin(\beta z)\sin(\pi y/h), \end{aligned} \tag{1}$$

where A is the forcing amplitude and β the wavenumber along z. The wavenumber was chosen such as to have vortex periods $\Lambda = 2\pi/\beta$ between $1.1h$ and $9.9h$, corresponding to inner-scaled wavelengths Λ^+ between 120 and 3630. Here and in

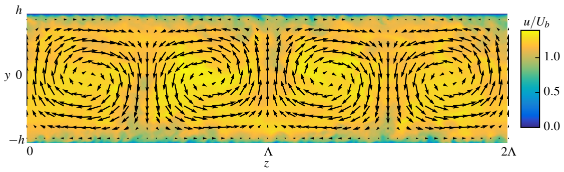

Figure 1: Instantaneous flow field of a controlled simulation for $Re_\tau = 550$ illustrating the large-scale vortices. The figure depicts two vortex wavelengths, with $\Lambda = 3.3h$, on a cross-stream channel plane coloured by streamwise velocity magnitude. The control amplitude is $\max|\langle v\rangle_{x,t}| \approx 0.07U_b$.

the following, all inner-scaled quantities are referred to the uncontrolled case and are indicated with a plus sign, *i.e.* $(\cdot)^+$. A sketch of the control vortices for $\Lambda = 3.3h$ is depicted in Figure 1. Since A does not correspond to a measurable flow quantity, the maximum wall-normal mean velocity is used to characterise the strength of the vortices, *i.e.* $\max|\langle v\rangle_{x,t}|/U_b$, where $\langle\cdot\rangle_{x,t}$ denotes the average in the streamwise direction and time.

ANALYSIS AND RESULTS

A total of 222 controlled simulations have been performed varying the Reynolds number, the control amplitude and the wavelength of the vortices. As shown in Ref. [1], the control scheme is effective at both $Re_\tau = 104$ and 180. For these values of the Reynolds number a drag reduction of up to 16% and 18%, respectively, can be achieved. The performance of the large-scale vortices, though, degrades rapidly: for $Re_\tau = 360$ the maximum DR is only 8%, and for $Re_\tau = 550$ no more than $0.4\% \pm 0.28\%$ can be obtained [2]. The present analysis covers the entire range of control amplitudes and reasonable vortex wavelengths, the drag reduction values presented are, therefore, the highest achievable under optimal conditions. This result is in agreement with Ref. [4], which shows that selectively damping small-scale fluctuations in a turbulent channel flow for $Re_\tau = 640$ is more effective than damping their large-scale counterparts, albeit their control strategy is different from the present approach based on Ref. [16].

The drag reduction including its uncertainty is illustrated in Figure 2 where panel (a) (in semi-log scale) shows the maximum achievable value of DR as a function of the Reynolds number. Panels (b–e) show the details at each Reynolds number by presenting the performance of the control strategy for $Re_\tau = 104, 180$ and 360 as a function of forcing amplitude and vortex wavelength. Since the method under investigation is an active control scheme, the power used to generate and sustain the large-scale vortices needs to be taken into account for a complete assessment of the performance. The net power saving rate is defined as $S = (P_{\text{unc}} - P_{\text{con}})/P_{\text{con}} = \text{DR} - P_{\text{in}}/P_{\text{unc}}$, where P_{unc} is the power required to drive the uncontrolled channel flow, while P_{in} is the power needed by the control, computed for an ideal actuator as $P_{\text{in}} = 1/(\Omega T)\int_\Omega \int_0^T \boldsymbol{f}\cdot\boldsymbol{v}\,\mathrm{d}t\,\mathrm{d}\Omega$. As it can be observed in Figure 2(a), the Reynolds-number dependence of this figure of merit is qualitatively similar to that of DR, confirming that the large-scale vortices perform well for low Reynolds numbers but fail to provide a positive effect for $Re_\tau > 550$. In particular, it was observed that the energy consumed by the ideal actuators does not significantly affect the parameters for the control: both the optimal wavelength and the forcing amplitude exhibit the same values compared to when not considering the power used to generate the large-scale vortices.

The final contribution will include a complete study on the causes that lead the method to become ineffective for high *Re*. Different aspects of the interaction between the control mechanism and the underlying flow will be analysed in order to shed light on the DR(*Re*) trend.

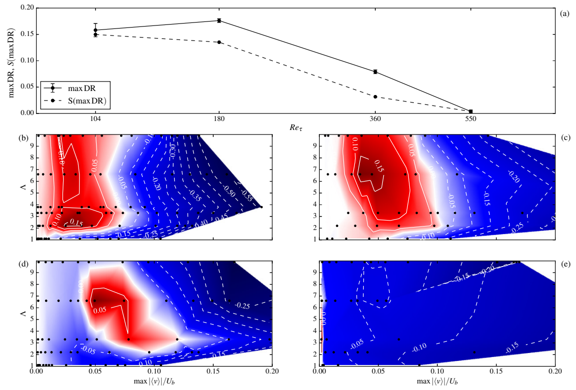

Figure 2: Panel (a): maximum achievable drag reduction as a function of friction Reynolds number (continuous line) and corresponding net power saving (dashed line). The x-axis is in logarithmic scale. Panels (b) to (e) depict DR as a function of control strength, $\max|\langle v\rangle_{x,t}|/U_b$, and wavelength of the vortices, Λ. $Re_\tau = 104, 180, 360$ and 550 are reported in (b), (c), (d) and (e), respectively. In (b–e) red and blue colours correspond to interpolated positive, resp. negative, values (reported as labels on the isocontours) of DR, based on the simulations indicated through black points.

REFERENCES

[1] J. Canton, R. Örlü, C. Chin, N. Hutchins, J. Monty, and P. Schlatter. *Flow, Turbul. Combust.*, 97:811–827, 2016.

[2] J. Canton, R. Örlü, C. Chin, and P. Schlatter. *Phys. Rev. Fluids*, 1:081501(R), 2016.

[3] M. Chevalier, P. Schlatter, A. Lundbladh, and D. S. Henningson. SIMSON - A pseudo-spectral solver for incompressible boundary layer flows. Technical Report TRITA-MEK 2007:07, KTH Mechanics, Stockholm, Sweden, 2007.

[4] K. Fukagata, M. Kobayashi, and N. Kasagi. *J. Fluid Sci. Technol.*, 5:574–584, 2010.

[5] M. Gad-el Hak. *Flow Control: Passive, Active, and Reactive Flow Management*. Cambridge University Press, 2007.

[6] R. García-Mayoral and J. Jiménez. *Phil. Trans. R. Soc. A*, 369:1412–1427, 2011.

[7] D. Gatti and M. Quadrio. *J. Fluid Mech.*, 802:553–582, 2016.

[8] E. Hurst, Q. Yang, and Y. M. Chung. *J. Fluid Mech.*, 759:28–55, 2014.

[9] K. Iwamoto, Y. Suzuki, and N. Kasagi. *Int. J. Heat Fluid Flow*, 23:678–689, 2002.

[10] Y. Kametani, K. Fukagata, R. Örlü, and P. Schlatter. *Int. J. Heat Fluid Flow*, 55:132–142, 2015.

[11] N. Kasagi, Y. Suzuki, and K. Fukagata. *Annu. Rev. Fluid Mech.*, 41:231–251, 2009.

[12] S. J. Kline, W. C. Reynolds, F. A. Schraub, and P. W. Runstadler. *J. Fluid Mech.*, 30:741–773, 1967.

[13] E. Moreau. *J. Phys. D. Appl. Phys.*, 40:605–636, 2007.

[14] R. D. Moser, J. Kim, and N. N. Mansour. *Phys. Fluids*, 11:943–945, 1999.

[15] M. Quadrio, P. Ricco, and C. Viotti. *J. Fluid Mech.*, 627:161–178, 2009.

[16] W. Schoppa and F. Hussain. *Phys. Fluids*, 10:1049, 1998.